Conformational Studies on Peptides as Enzyme Inhibitors: Chymotrypsin Inhibitors Using Bowman–Birk Type as Models

Vincenzo Pavone,[a] Carla Isernia,[a] Michele Saviano,[a] Lucia Falcigno,[a] Angelina Lombardi,[a] Livio Paolillo,[a] Carlo Pedone,[a] Solfrid Buøen,[b] Hilde Merete Naess,[b] Hege Revheim[b] and Jon Amund Eriksen[b]

[a] *Centro Interdipartimentale di Ricerca su Peptidi Bioattivi, University of Naples 'Federico II', via Mezzocannone 4, 80134 Napoli, Italy*

[b] *Norsk-Hydro a.s. Research Centre Porsgrunn, PO Box 2560, N-3901, Norway*

A complete structural characterization in solution, by NMR spectroscopy, and *in vacuo*, by molecular dynamic simulations, of two synthetic peptide fragments from SBBI (Soybean Bowman–Birk Inhibitor) is reported. Peptide 197, corresponding to the SBBI(41–49) chymotrypsin recognition site, has free N- and C-terminal groups, while peptide 212, corresponding to the Leu 16-SBBI(14–22) has uncharged and fully protected terminal ends. Peptide 212 shows significant anti-chymotryptic activity while peptide 197 is inactive. Neither of the two peptides shows anti-tryptic activity. The structural information obtained in the present paper suggests a quantitative structure–activity relationship which may help both in understanding the mechanism of action of protease inhibitors, and in providing new directions for the rational design of more specific and potent inhibitors.

In recent years considerable attention has been devoted to the understanding of the mechanism of action of serine-protease inhibitors at a molecular level.[1–8] In particular, information about trypsin and chymotrypsin vegetable inhibitors has been growing[9–11] and at the same time detailed structural information from X-ray diffraction analysis and NMR spectroscopy has become available.[12–27]

Proteins belonging to the Bowman–Birk family of double headed protease inhibitors (BBIs), found in plant seeds, and particularly in legume seeds,[9] have also been studied in detail.[9–11,28–34] BBIs are characterized as single chain proteins with seven disulfide bridges with molecular weight of 8–9 kDa. There are two inhibitor sites located in two separate loops at opposite ends of the folded protein. Each loop, formed by one disulfide bridge, usually includes nine amino acid residues.[9–11] X-Ray crystallography of the BBI-trypsin complex revealed that only residues belonging to the nine membered loop are in direct contact with the enzyme.[29] In addition the cyclic nona-peptides, corresponding to the active loops of BBI, have been shown to be relatively strong enzyme inhibitors.[35–37]

Soybean BBI shows independent anti-tryptic and anti-chymotryptic activity. With respect to the anti-tryptic activity position 16 is the location of P_1, using the notation of Schechter and Berger.[38] The specificity of many serine-protease inhibitors can be manipulated by alteration of the amino acid in P_1.[39–42] This has also been shown for synthetic peptides corresponding to the anti-tryptic loop SBBI(14–22) Cys-Thr-Lys-Ser-Asn-Pro-Pro-Gln-Cys. Replacement of Lys16 by Leu in SBBI(14–22) results in an anti-chymotryptic peptide.[36] Furthermore Leu16-SBBI(14–22) has been found[36] to be a chymotrypsin inhibitor ten times stronger than the peptide corresponding to the anti-chymotryptic loop SBBI(41–49) Cys-Ala-Leu-Ser-Tyr-Pro-Ala-Gln-Cys. Furthermore, recent studies[43] have shown that the binding loops (14–22) and (41–49) of SBBI are active peptide inhibitors especially when the N- and C-terminal ends are devoid of charges as in the acetyl-amide form.

Several attempts have been made to optimize the inhibitor activity of derived BBI synthetic cyclic peptides.[36,37,43–45] A SAR (Structure–Activity Relationship) study, which in our opinion could be helpful in understanding inhibitor–substrate differences, has not been reported to our knowledge for any of the quoted synthetic peptides. A recent report[43] on the BBI(D4) loop 19–31 indicates that the inhibitory activity of BBIs is the result of a conformationally rigid loop structure.

With the aim of a better understanding of the conformational features necessary in the inhibitory process, we have undertaken a systematic structural analysis on four cyclic nona-peptides, derived from the anti-tryptic and the anti-chymotryptic loops of SBBI.

NMR spectroscopy in solution coupled to MD (Molecular Dynamic) simulations *in vacuo* were used in order to evaluate conformational preferences.

This first report concerns the structural characterization in solution of two cyclic nona-peptides as chymotrypsin inhibitors, namely (peptide 197)

H–Cys-Ala-Leu-Ser-Tyr-Pro-Ala-Gln-Cys–OH and

Ac–Cys-Thr-Leu-Ser-Asn-Pro-Pro-Gln-Cys–NH_2 (peptide 212). A second report[46] will discuss the structural analysis in solution of the peptidic trypsin inhibitors

H–Cys-Thr-Lys-Ser-Asn-Pro-Pro-Gln-Cys–OH and

Ac–Cys-Thr-Lys-Ser-Asn-Pro-Pro-Gln-Cys–NH_2.

Experimental

Peptide Synthesis.—The peptides were synthesized by using the fmoc/*tert*-butyl (fmoc, fluoren-9-ylmethoxycarbonyl) protecting group strategy in continuous flow solid phase peptide synthesis,[47] performed by an automated Biolynx 4170 peptide synthesizer upgraded to a Nova Syn Crystal peptide synthesizer (Novabiochem UK). The fmoc-amino acid derivatives were activated[48] for coupling by tbtu [2-(1*H*-benzotriazol-1-yl)-1,1,3,3-tetramethyluronium tetrafluoroborate]. Four equivalents of activated amino acid derivatives were used in each coupling step. Side chain protection during the synthesis was as follows: Asn(trt), Cys(trt), Gln(trt), Lys(*t*-boc), Ser(Bu^t), Thr(Bu^t) Tyr(Bu^t) (trt, triphenylmethyl; *t*-boc, *tert*-butoxycarbonyl; Bu^t, *tert*-butyl). Novasyn PA 500 resin was used to prepare peptides with a free C-terminal and peptides with C-terminal amides were obtained by using Novasyn PR 500 resin. (All amino acid derivatives, resins and tbtu were purchased from Novabiochem). DMF (dimethylformamide; Fluka) was used as

solvent and fmoc cleavages were performed by 20% piperidine (Fluka) in DMF. *N*-Terminal acetylation of the peptides was performed on the resin by treatment with five equivalents of acetic acid anhydride (Fluka) and two equivalents of diisopropylethylamine (Fluka) dissolved in DMF. 5% Ethanedithiol (Fluka) in trifluoroacetic acid (Fluka) was used to remove side chain protecting groups and to cleave the linear peptides from the resin. The peptides were purified by semi-preparative reverse phase (C-18) HPLC (high performance liquid chromatography) using a Shimadzu LC8A chromatograph and cyclized[49] by treatment in a mixture of DMSO (dimethylsulfoxide; Fluka), acetic acid (Fluka) and H_2O at pH 6. Completion of the reaction was monitored by analytical reverse phase (C-18) HPLC (Shimadzu LC8A) and Ellman's test.[50] The cyclic peptides were purified by reverse phase (C-18) HPLC and lyophilized. The purity of the peptides was determined by analytical reverse phase (C-18) HPLC.

Inhibitor Activity.—The anti-chymotryptic and anti-tryptic activity of the peptides were determined by using respectively *N*-α-L-Tyr ethyl ester (256 nm) and *N*-α-L-Arg ethyl ester (253 nm) as substrates in standard enzyme assays.[51]

NMR Spectroscopy.—^{1}H NMR 1D and 2D experiments were recorded on a VARIAN UNITY 400 spectrometer, operating at 400 MHz and equipped with a SPARC Station SUN 330, located at the *Centro Interdipartimentale di Ricerca su Peptidi Bioattivi*, of the University *Federico II* of Naples.

NMR samples were prepared by dissolving 3–4 mg of peptide in 0.5–0.6 cm^3 of [$^2H_6$]DMSO (Aldrich, isotopic purity 100%). Chemical shifts were referred to internal TMS (tetramethylsilane). All experiments were performed at 298 K.

Phase sensitive DQFCOSY (Double Quantum Filtered Correlated Spectroscopy),[52] HOHAHA (Homonuclear Hartmann–Hahn Spectroscopy),[53] NOESY (Two-Dimensional Nuclear Overhauser Enhancement Spectroscopy),[54] and ROESY (Two-Dimensional Rotating Frame Overhauser Enhancement Spectroscopy)[55] techniques were used applying the States–Haberkorn method. Typically 40–64 scans were recorded with 512 × 2k data points (512 × 4k for the DQFCOSY). NOESY spectra were collected with a mixing time of 250 ms and the HOHAHA experiments were recorded with a mixing of 70 ms. A continuous spin-lock was used for the ROESY spectra (mixing time 120 ms); off-resonance effects have been compensated using two 90° hard pulses, before and after the spin-lock time.[56] The FIDs were multiplied by suitable weighting functions and zero-filled to 1k data points in F_1 prior to Fourier transformation.

Cross-peak intensities in the NOESY spectra were measured by volume integration using the VARIAN software.

Calculations.—Energy minimization and RMD (Restrained Molecular Dynamics) simulation were performed with a Personal Iris 4D25 Turbo Silicon Graphics workstation, using the DISCOVER program ver.2.8 developed by BIOSYM TECHNOLOGIES with the Consistent Valence Force field[57–59] (CVFF). The equations of motion were solved using the so-called Leapfrog integration algorithm,[60] with a time step of 0.5 fs.[61]

Solvent molecules were not explicitly included in the simulations, but the solvent screening was implicitly modelled, by adjusting the dielectric constant behaviour[62] using the so-called 'distance dependent dielectric' function. For each simulation, carried out *in vacuo*, the computational conditions were chosen to avoid boundary effects.[63]

The distance restraint was given by a skewed biharmonic potential added to the total energy of the system.[64] The dihedral angle constraints were not used since the measured $^3J_{NH-\alpha CH}$ coupling constants were consistent with multiple φ values.

The initial structures were built using standard parameters supplied by the INSIGHT software package.[65] These structures were subjected to a simulated annealing procedure using the NOE (Nuclear Overhauser Enhancement) effects to bias the trajectory into a reduced area. The structures best satisfying distances and dihedral angles derived from NMR data, were subjected to the RMD with the following protocols. Each system was relaxed to eliminate hot spots, performing approximately 100 steps of energy minimizations[66] using the conjugate gradient method,[67] before RMD were run on resulting models. The energy-minimized structures were used as the initial structures for the RMDs *in vacuo* at 300 K.

In each simulation, the system was equilibrated for 30 ps, then an additional 40 ps of simulation without rescaling was carried out, since energy conservation was observed and the average temperature remained essentially constant around the target value of 300 K.

The average structures were then checked for consistency with all observable NOEs. Coordinates and velocities for the simulations were dumped to a disk every 10 steps during the last 20 ps of the simulations. The dumped data were used for the analyses. The energy minimization procedure was applied several times during the equilibrium phase of the RMD simulations in order to search conformations closer to the 'global minimum'.[67]

Results and Discussion

The purity of the synthetic peptides was >95% as ascertained by HPLC. Neither anti-chymotryptic nor anti-tryptic activity was detected for peptide 197. Peptide 212 shows significant anti-chymotryptic activity. The calculated inhibition constant (k_i) for peptide 212 with respect to chymotrypsin was 25×10^{-6} mol dm^{-3}.

The NMR spectra of peptide 197 *cyclo*-[H–(Cys-Ala-Leu-Ser-Tyr-Pro-Ala-Gln-Cys)–OH] showed more resonances than expected. NOESY and ROESY cross peaks appeared to be the same and revealed the presence of two conformational families in slow exchanging equilibrium (relative population 55:45, conformer II : conformer I).

The identification of the spin systems belonging to the two conformers was accomplished through homonuclear correlation experiments. The spin systems were then sequentially assigned from the NOE effects between resonances of adjacent residues. Two regions of the 250 ms NOESY spectrum are shown in Fig. 1.

Proton chemical shifts, temperature coefficients of amide protons and $^3J_{NH-\alpha CH}$ coupling constants for both conformers are listed in Tables 1 and 2. Chemical shift values,[68] indicative of random structures, do not correspond to those observed (*i.e.* Ala2 NH, Ser4 NH) for peptide 197. In addition considerable differences are observed for Pro6 and for the adjacent residues, in comparing chemical shifts of conformer I and II. The δ protons of Pro6 show an unusual highfield chemical shift in conformer I. The δ values for the amidic protons of Tyr5 and of Ala7 are shifted upfield by approximately 0.9 and 0.5 ppm.

In the ROESY spectrum, exchange signals belonging to the two conformers (*i.e.* 4.23/3.76 ppm α-protons of Pro6 in the two conformers), as well as ROESY cross-peaks due to spatial interactions within each conformer, were clearly observable.

The NOE contacts between the α-proton of Tyr5 and δδ′-protons of the Pro6,[69] as well as the NOE between α-Tyr5 and α-Pro6, are diagnostic for the evaluation of the structural diversity of the two conformational families. The most abundant conformation (conformer II) is characterized by all

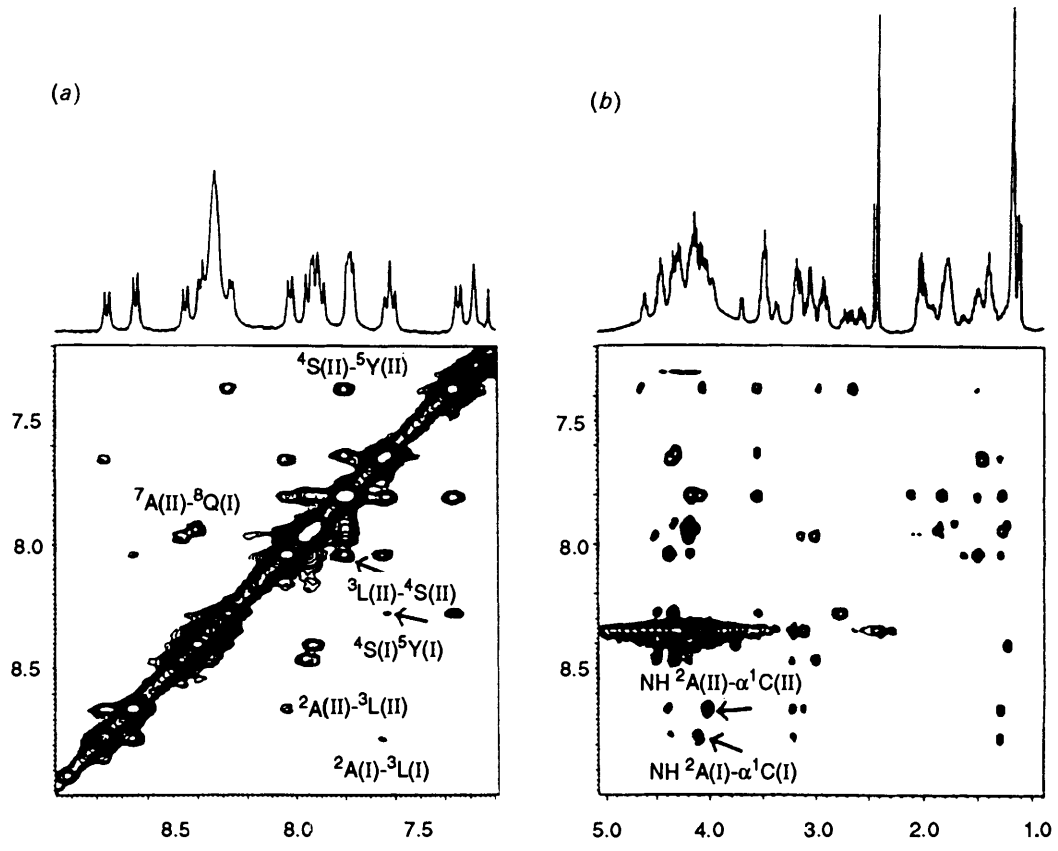

Fig. 1 Peptide 197 400 MHz 250 ms NOESY spectrum: (*a*) NH–NH region; (*b*) NH-aliphatic region. Relevant correlations are labelled.

trans peptide bonds. The minor conformer (I) has instead a *cis* peptide bond between Tyr5 and Pro6.

NOE effects of αC_iH–$N_{i+1}H$ type are all observed, while weak N_iH–$N_{i+1}H$ inter-residue correlations are present in the Ala2-Tyr5 region. A NOE contact between NHAla7-NHGln8 is also revealed in conformer I.

Temperature coefficients of amide NHs (Table 2) are rather different for each residue indicating a different solvent shield and a possible involvement in hydrogen bond of the Ala2 NH in conformer I and of the Gln8 NH in conformer II. A low value for Cys1 NH in peptide 197 can tentatively be attributed to the protonation state and ion-pairing, while for peptide 212 to hydrogen bonding.

Backbone coupling constants $^3J_{NH-\alpha CH}$ for both conformers (Table 2) are relatively high with the exception of Tyr5 in conformer I.

The small differences in $^3J_{\alpha CH-\beta CH}$, $^3J_{\alpha CH}$, $^3J_{\alpha CH-\beta'CH}$ coupling constants (Cys1: $^3J_{\alpha\beta} = 6.5$ Hz in both conformers, $^3J_{\alpha\beta'} = 8.0$ Hz in conformer I and 6.5 Hz in conformer II; Cys9: $^3J_{\alpha\beta} = 5.6$ and $^3J_{\alpha\beta'} = 7.5$ Hz in conformer I, $^3J_{\alpha\beta} = {}^3J_{\alpha\beta'} = 7.3$ Hz in conformer II), as well as the partial Cys ββ′ signal overlap in the two conformers do not allow prochiral assignments of βCH_2 protons for both Cys1 and Cys9. Therefore, it was not possible to gain structural information on χ^1 and χ^2 angles for these residues. The ambiguity on ±90° torsion angle around the –S–S– bond could not be resolved. In agreement with the previous observations it can be hypothesized that the $^3J_{\alpha CH-\beta CH}$, $^3J_{\alpha CH-\beta'CH}$ coupling constants, both for Cys1 and Cys9, correspond to a mean value between those expected for staggered conformations and that the –S–S– bridge is free to move between two possible conformations.

In the case of peptide 212 *cyclo*-[Ac–(Cys-Thr-Leu-Ser-Asn-Pro-Pro-Gln-Cys)–NH_2] two or more conformers arising from *cis*/*trans* isomerization around the proline residues are also present in solution. The minor isomers that exhibit some resolved resonances have been integrated and each amount to approximately 5% of the major isomer (about 80%). No exchange peaks were observed in the ROESY spectrum, indicating a very slow exchange on the NMR time scale.

Sequential assignment of the main conformer was obtained by TOCSY, NOESY, ROESY and DQFCOSY experiments following the well-known protocol.[68]

Table 3 presents the proton chemical shifts; αCH proton resonances of Cys1, Pro6 and Cys9 residues exhibit unusual downfield shift.[68]

Backbone coupling constants are always in the range of 9–10 Hz (Table 3).

NOE contacts reveal a structure marked by a *cis* Asn5-Pro6 peptide bond (αCH Asn5-αCH Pro6) and by a *trans* Pro6-Pro7 bond (αCH Pro6-δδ′CH Pro7).

All sequential NOE contacts αC_iH–$N_{i+1}H$ are observed; weaker contacts N_iH–$N_{i+1}H$ also appear between Cys1-Gln8, Leu3-Ser4 and Ser4-Asn5 residues. A strong contact is present between the αCH protons of Cys1 and Cys9.

The NH temperature coefficient (Table 3) of Ser4 is very low and points to a structure where this NH is strongly solvent shielded and presumably forms an internal hydrogen bond. The Gln8 NH also shows a relatively low value (-2.0 ppbK^{-1}) of the temperature coefficient.

As far as the possible structural information on the cysteine sidechains is concerned, we cannot unequivocally determine the χ^1 and χ^2 angles, as already described for peptide 197. The $^3J_{\alpha\beta}$ and $^3J_{\alpha\beta'}$ coupling constants are 10 Hz and 6.0 Hz for Cys1, respectively, and 8.0 Hz for Cys9.

In addition, the NMR experiments were also performed in water solution. A preliminary analysis indicates a very similar magnetic behaviour. From a structural point of view it appears that both *cis* and *trans* isomers are present for peptides 197 and 212.

Restrained Molecular Dynamics were performed in two

Table 1 Peptide 197 proton chemical shifts (ppm) for both conformers I and II

AA	H	I	II
Cys1	NH	8.35	8.33
	αCH	4.11	4.07
	ββ'CH_2	3.22; 3.11	3.22; 3.11
Ala2	NH	8.77	8.66
	αCH	4.39	4.39
	βCH_3	1.29	1.29
Leu3	NH	7.65	8.02
	αCH	4.31	4.17
	ββ'CH_2	1.47	1.49
	γCH	1.47	1.49
	δδ'CH_3	0.84	0.87
Ser4	NH	7.62	7.80
	αCH	4.35	4.08
	ββ'CH_2	3.56	3.55
	OH	9.3 (9.15)*	9.3 (9.15)*
Tyr5	NH	8.27	7.36
	αCH	4.50	4.65
	ββ'CH_2	2.77	2.98; 2.65
	2,6H	6.98	7.00
	3,5H	6.68	6.61
Pro6	αCH	3.77	4.23
	ββ'CH_2	1.89; 1.35	2.00
	γγ'CH_2	1.55	1.88
	δδ'CH_2	3.25	3.57; 3.43
Ala7	NH	8.40	7.93
	αCH	4.16	4.14
	βCH_3	1.23	1.27
Gln8	NH	7.91	7.79
	αCH	4.32	4.18
	ββ'CH_2	1.84	1.82
	γγ'CH_2	2.09; 1.71	2.11
	δδ'NH_2	7.15; 6.76	7.29; 6.82
Cys9	NH	8.46	7.96
	αCH	4.50	4.51
	ββ'CH_2	3.24; 3.00	3.14; 3.02

* Resonances not assigned to conformer I or II.

Table 2 Peptide 197 temperature coefficients $\Delta\delta/\Delta T$ (ppb K^{-1}) of amidic protons and coupling constants $^3J_{NH-\alpha CH}$ (Hz) for conformers I and II

	Conformer I		Conformer II	
AA	$\Delta\delta/\Delta T$	$^3J_{NH-\alpha CH}$	$\Delta\delta/\Delta T$	$^3J_{NH-\alpha CH}$
Cys1	−1.9	—	−1.9	—
Ala2	0	7.8	−4.2	7.1
Leu3	+3.8	9.0	−3.5	6.6
Ser4	−6.6	9.0	—	7.7
Tyr5	−7.5	4.9	−2.8	8.3
Ala7	−3.5	7.1	−4.2	6.4
Gln8	−5.0	8.7	−2.0	6.7
δδ'NH_2	−3.8; −5.1		−4.8; −5.5	
Cys9	−4.6	8.0	−2.7	8.3

stages. The first one generates conformations that are consistent with the NOE measured distances. In this step two possible peptide structures were built on the basis of ±90°–S–S– dihedral angle. The analysis of the annealing stage shows that for peptide 197, in either *cis* or *trans* conformation of the Tyr5-Pro6 peptide bond, both the –S–S– dihedral angles are compatible with NMR data. On the contrary, for peptide 212 the value of +90° is the only one compatible with the experimental data.

In the second step five RMD simulations (one for each model) *in vacuo* at 300 K were carried out: energy minimizations were repeated using as a starting point intermediate coordinates of each RMD simulation; many local minima were obtained with almost comparable energy. Similarity of the structures mini-

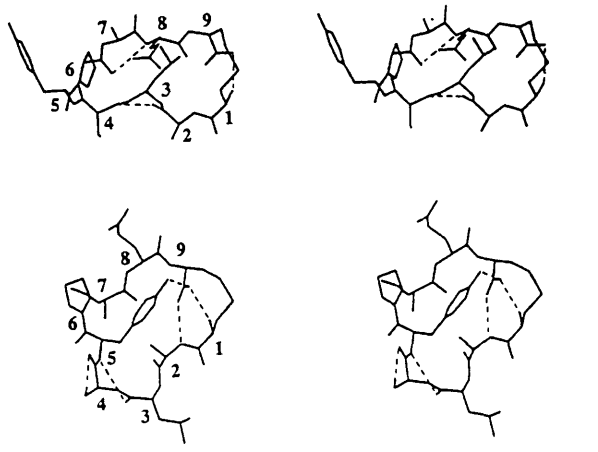

Fig. 2 Stereo view of the average models for peptide 197 (conformer I). Top: model with −90°–S–S– bond; bottom: model with +90°–S–S– bond. The intramolecular hydrogen bonds are indicated as dashed lines. Residues are sequentially labelled.

Fig. 3 Stereo view of the average models for peptide 197 (conformer II). Top: model with –90°–S–S– bond; bottom: model with +90°–S–S– bond. The intramolecular hydrogen bonds are indicated as dashed lines. Residues are sequentially labelled.

mized along the trajectory was evaluated by comparing the RMS deviation of the C^α atoms for each possible pair of structures. The analysis of each set of these minimized structures revealed the existence of only one conformational family for each starting model.

In particular peptide 197 was subjected to four simulations. The analysis of the dumped data showed average structures compatible with the NMR data. Time averaged structures for the two simulations of peptide 197 (conformer I) and for the two simulations of peptide 197 (conformer II) are reported in Figs. 2, 3 and in Table 4.

The analysis of the two average structure models, differing for the –S–S– torsion angle, shows that these models have two different overall shapes. In fact, major differences are observed in the Ala2-Ser4 peptide segment; these also may imply different hydrogen bonds (Table 5).

As far as conformer II is concerned taking into account the existence of a *trans* Tyr5-Pro6 peptide bond, the analysis of RMD data shows that the two average models are quite similar, with the noticeable difference only in the Gln8-Cys9 segment, due to the different –S–S– dihedral angle. This similarity can be extended to the spatial distribution of side chains. In addition,

Table 3 Peptide 212 proton chemical shifts (ppm), temperature coefficients $\Delta\delta/\Delta T$ (ppb K^{-1}) of amidic protons and $^3J_{NH-\alpha CH}$ (Hz) coupling constants

AA	NH	αCH	βCH	γCH	Others	$\Delta\delta/\Delta T$	$^3J_{NH-\alpha CH}$
Cys1	8.43	5.28	2.90 2.84		1.93 Ac	−5.7	8.8
Thr2	8.43	4.16	4.16	1.19	—	−5.7	8.8
Leu3	8.35	4.32	1.55	1.55	0.88 0.78	−6.9	8.1
Ser4	7.18	4.20	3.74 3.42		—	−0.2	8.5
Asn5	8.24	4.93	2.74	2.17	7.36 γNH 6.79 γ'NH	−6.6 −4.1 (γNH) −4.8 (γ'NH)	9.6
Pro6		5.02	2.26	1.78 1.90	3.38		
Pro7		4.28	2.32	1.96 1.76	3.75 3.55		
Gln8	7.60	4.56	1.86	2.02 1.73	7.08 δNH 6.77 δ'NH	−2.2 −4.6 (δNH) −5.7 (δ'NH)	9.6
Cys9	8.82	5.07	2.89	7.54 CONH 7.33 CONH		−7.6 −3.5(CONH) −5.5(CONH)	9.7

Table 4 Dihedral angles in the peptide main chain for the average structures of peptide 197 [conformer I (*a*, *b*) and II (*c*, *d*)] as obtained from the MD simulations: (*a*, *c*) –S–S– dihedral value +90°, [*b*,*d*] –S–S– value −90°

	∠	Cys1	Ala2	Leu3	Ser4	Tyr5	Pro6	Ala7	Gln8	Cys9
(*a*)	φ	—	−80.0	−63.2	−100.1	−106.0	−71.5	−103.9	−131.7	−89.8
	ψ	−53.0	122.7	−23.7	81.1	154.9	119.3	100.7	60.0	140.0
	ω	−177.3	170.6	174.2	−165.9	−9.9	176.0	170.0	160.4	—
(*b*)	φ	—	−159.2	−88.6	−122.1	−132.3	−78.2	−85.7	−131.7	66.2
	ψ	−85.8	94.7	87.7	−107.4	118.2	163.5	87.0	85.6	174.0
	ω	−179.3	173.6	176.2	156.9	4.6	176.7	−161.0	167.7	—
(*c*)	φ	—	−127.4	−96.2	52.4	−138.5	−59.9	−97.0	−62.9	−80.1
	ψ	−55.0	161.4	101.2	81.0	124.7	−29.1	67.4	−171.4	−179.5
	ω	−164.1	−177.1	−177.3	−158.4	−169.1	−170.2	−174.3	160.8	—
(*d*)	φ	—	−104.8	−107.3	64.7	−150.6	−49.3	−105.6	−105.2	−90.3
	ψ	−45.0	143.4	97.2	76.2	131.9	−40.0	84.5	144.7	152.9
	ω	180.0	−173.0	−175.5	177.7	−170.6	177.4	−158.9	163.2	—

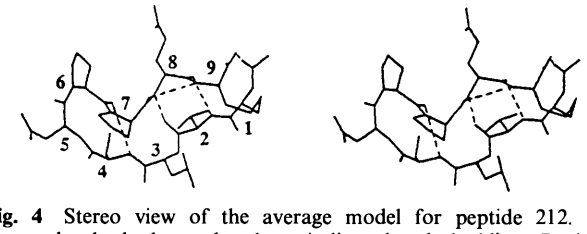

Fig. 4 Stereo view of the average model for peptide 212. The intramolecular hydrogen bonds are indicated as dashed lines. Residues are sequentially labelled.

the two conformations also appear to have similar hydrogen bonds (Table 5).

Furthermore the simulation carried out on a single model for peptide 212 (containing a +90° –S–S– bond and a *cis* Asn5-Pro6 peptide bond) gives an average structure (Fig. 4) whose conformational parameters are reported in Table 6. The analysis of the dumped data shows that this structure is consistent with the NMR data. In particular the simulation gives an explanation both of the high temperature coefficients, but for Ser4, and of the *J* coupling constants. The Ser4 NH is in fact involved in a hydrogen bond with a N • • • O=C distance of 3.0 Å, as reported in Table 6. It is interesting to compare this structure with the *cis* conformer containing the same value of –S–S– dihedral angle found for peptide 197. The two structures exhibit a considerable similarity, with comparable values of the dihedral angles.

In conclusion, the NMR studies in combination with molecular dynamic simulations indicate that all the examined peptides show conformational flexibility in DMSO solution. Peptide 197 at 298 K exists as two conformers in relative concentration 55:45. Peptide 212 has one predominant

conformer, with minor fractions amounting to less than 20%. For these reasons a full conformer analysis has been carried out only for peptide 197 while in the other case only the predominant conformer has been characterized. This flexibility can be attributed, for both compounds, to a *cis–trans* isomerism around the Xaa-Pro peptide bond and tentatively to the possible isomerism from +90° to −90° of the disulfide bridge. The motion of these two parts of the molecules might be co-operative.

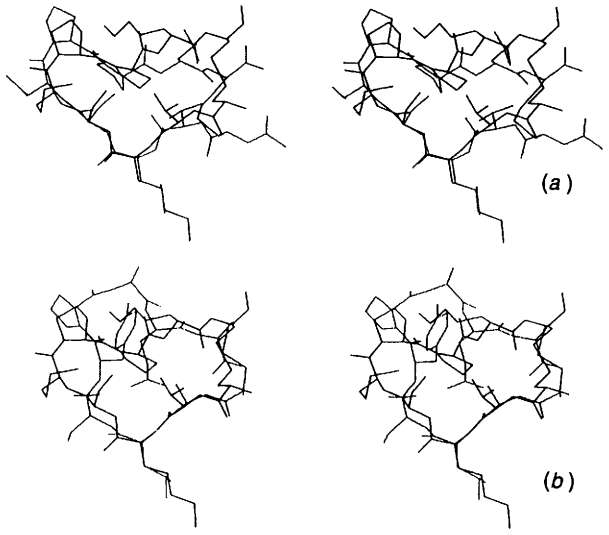

Fig. 5 Stereo view of the superimposition of BBI site (1TAB: I14–I22) (filled line) with the average models (dotted line) (*a*) for peptide 212 and (*b*) for peptide 197 (conformer I) with a +90° S–S bond

Table 5 Intramolecular hydrogen bond as obtained from the MD simulations for peptide 197: (*a*) conformer I with +90° of the –S–S– torsion angle, (*b*) conformer I with −90° of the –S–S– torsion angle, (*c*) conformer II with +90° of the –S–S– torsion angle, (*d*) conformer II with −90° of the –S–S– torsion angle

	Donor	Acceptor	Distance Å
(*a*)	NHAla2	COCys9	2.9
	NHCys1	COCys9	2.7
	NHThr5	COLeu3	3.5
	OγSer4	COSer4	3.0
	OεThr5	COCys9	3.1
(*b*)	NHCys1	COCys9	2.7
	NHGln8	COPro6	3.3
	NHLeu3	COAla2	3.4
(*c*)	NHCys1	COCys9	2.7
	NHεGln8	COAla2	2.8
	NHSer4	COAla2	3.5
	OγSer4	COLeu3	2.7
	OγSer4	COSer4	2.9
	NHTyr5	OεGln8	3.2
	NHGln8	COTyr5	3.2
(*d*)	NHCys1	COCys9	2.7
	NHAla2	COCys9	2.9
	OγSer4	COLeu3	2.6
	NHSer4	OεGln8	3.3

It is interesting to note that peptides 197 and 212 show a different degree of flexibility. Peptide 197 seems to be the most flexible: two almost equally abundant conformational families are observed in DMSO solution; the NOE effects are consistent with four possible overall shapes of the molecules corresponding to a combination of *cis*/*trans* peptide bond configuration around the Tyr5-Pro6 and to +90° and −90° of the –S–S– bond. Peptide 212 is structurally more rigid: a major conformational component is observed in solution; the NOE effects are consistent with only a *cis* Asn5-Pro6 *cis* configuration and a + 90° –S–S– torsion angle.

These findings seem to correlate well with the observed inhibitory activity of both molecules. The structural similarities can be seen from Fig. 5 where the protein segment 1TAB: I14–I22, obtained from the Protein Data Bank [70,71] at Brookhaven National Laboratory, is superimposed with peptide 212 and the *cis* conformer of peptide 197 with –S–S– bond +90°.

Therefore it is likely to hypothesize that in a serine-protease inhibitor, as in the case of BBI, BPTI (Bovine Pancreatic Trypsin Inhibitor), CI-2 (Chymotrypsin Inhibitor-2), Eglin-c and OMTKY3 (Turkey Ovomucoid Third Domain), the small recognition site, within the protein sequence, is frozen in the appropriate conformation by the rest of the polypeptide chain. When the peptidic region of the inhibitor, directly interacting with the enzyme, is isolated from the rest of the molecule, as in the case of synthetic peptide models, three major structural changes occur: (i) two opposite terminal charges are introduced in the molecule; (ii) the terminal residues may be free to move; (iii) many long range interactions, present in the protein structure are missing in the peptide models. These observations may explain both the different conformational behaviour of the synthetic peptide model, as in the case of the molecules presently investigated, and the different inhibition activity. Finally, the rigidity of the enzyme complementary site should prevent the scissile peptide bond from reaching a position close enough to the nucleofile Ser195 γO atom to start the hydrolytic reaction. Further studies on different cyclic peptide inhibitors of other serine-proteases are presently in progress.

Acknowledgements

We wish to thank Mr. Marco Mammucari, Miss Gabriella De Vita, Miss Hilde Asheim, Miss Guri Basma for technical assistance and Mrs. Gerd Aasen for enzyme assays performance.

Table 6 Dihedral angles in the peptide main chain and intramolecular hydrogen bonds for the average structure of peptide 212 as obtained from the MD simulations with –S–S– dihedral value at +90°

	Cys1	Thr2	Leu3	Ser4	Asn5	Pro6	Pro7	Gln8	Cys9
φ	−128.5	−142.4	−81.5	−139.4	−145.3	−58.6	−82.4	−107.6	−104.2
ψ	114.4	100.0	106.9	−112.1	101.1	149.4	93.4	81.1	108.7
ω	175.6	−169.6	164.0	173.5	−1.6	166.9	−167.7	174.7	—

Donor	Acceptor	Distance Å
NHCys1	COCys9	3.1
NHThr2	COGln8	3.6
NHCys9	COPro7	3.7
NHSer4	COPro6	3.0
NHGln8	COThr2	3.7

References

1 R. Huber and W. Bode, *Acc. Chem. Res.*, 1978, **11**, 114.
2 M. Jr. Laskowski and I. Kato, *Annu. Rev. Biochem.*, 1980, **49**, 593.
3 M. Bolognesi, P. Ascenzi, G. Amiconi, E. Menegatti and M. Guarneri, in *Macromolecular Biorecognition*, eds. I. Chaiken, E. Chaincone, A. Fontana and P. Neri, Humana Press, Clifton, 1988, p. 81.
4 P. Ascenzi, G. Amiconi, M. Bolognesi, E. Menegatti and M. Guarneri, *J. Mol. Catal.*, 1988, **47**, 297.
5 P. Ascenzi, G. Amiconi, E. Menegatti, M. Guarneri, M. Bolognesi and H. P. Schnebli, *J. Enz. Inhibit.*, 1988, **2**, 167.
6 P. Ascenzi, M. Coletta, G. Amiconi, R. De Cristofaro, M. Bolognesi, M. Guarneri and E. Menegatti, *Biochim. Biophys. Acta*, 1988, **956**, 156.
7 P. Ascenzi, G. Amiconi, M. Bolognesi, E. Menegatti and M. Guarneri, *Biochim. Biophys. Acta*, 1990, **1040**, 134.
8 M. Jr. Laskowski, S. J. Park, M. Tashiro and R. Wynn, in *Protein Recognition of Immobilized Ligands*, ed. T. Hutkens, UCLA Symposia on Molecular and Cellular Biology, New Series, Alan R. Liss, Inc., New York, 1989, vol. 80, p. 149.
9 Y. Birk, in *Recent Advances in Research in Antinutritional Factors in Legume Seeds*, eds. Huisman and van den Poel, Liener Pudoc Wageningen, 1989, p. 83.
10 H. D. Belitz and J. K. P. Weder, *Food Rev. Int.*, 1990, **6**, 151.
11 M. Richardson, in *Methods in Plant Biochemistry*, ed. L. Rogers, Academic Press, New York, London, 1991, vol. 5, p. 259.
12 R. Huber, D. Kukla, W. Bode, P. Schwager, K. Bartels, J. Deisenhofer and W. Steigemann, *J. Mol. Biol.*, 1974, **89**, 73.
13 J. Deisenhofer and W. Steigemann, *Acta Crystallogr., Sect. B, Struct. Crystallogr.*, 1975, **31**, 238.
14 A. Wlodawer, J. Walter, R. Huber and L. Sjölin, *J. Mol. Biol.*, 1984, **180**, 301.
15 R. J. Read and M. N. J. James, in *Proteinase Inhibitors*, eds. A. J. Barrett and G. Salvesen, Elsevier, Amsterdam, 1986, p. 301.
16 M. Fujinaga, A. R. Sielecki, R. J. Read, W. Ardelt, M. Laskowski and M. N. G. James, *J. Mol. Biol.*, 1987, **195**, 397.
17 C. A. McPhalen and M. N. G. James, *Biochemistry*, 1987, **26**, 261.
18 A. Wlodawer, J. Nachman, G. L. Gilliland, W. Gallagher and C. Woodward, *J. Mol. Biol.*, 1987, **198**, 469.
19 S. Onesti, P. Brick and D. M. Blow, *J. Mol. Biol.*, 1991, **217**, 153.
20 F. Frigerio, A. Coda, L. Pugliese, C. Lionetti, E. Menegatti, G. Amiconi, H. P. Schnebli, P. Ascenzi and M. Bolognesi, *J. Mol. Biol.*, 1992, **225**, 107.
21 Y. Takeuchi, T. Nonaka, K. T. Nakamura, S. Kojima, K. Miura and Y. Mitsui, *Proc. Natl. Acad. Sci. USA*, 1992, **89**, 4407.
22 P. Brandt and C. Woodward, *Biochemistry*, 1987, **26**, 3156.
23 G. M. Clore, A. M. Gronenborn, M. Nilges and C. A. Ryan, *Biochemistry*, 1987, **26**, 8012.
24 G. Wagner, W. Braun, T. F. Havel, T. Schaumann, N. Go and K. Wütrich, *J. Mol. Biol.*, 1987, **196**, 611.
25 T. A. Holak, W. Bode, R. Huber, J. Otlewski and T. Wiluz, *J. Mol. Biol.*, 1989, **210**, 649.
26 S. L. Heald, R. F. Tilton, L. J. Hammond, A. Lee, R. M. Bayney, M. E. Kamarck, T. V. Ramabhadran, R. N. Dreyer, G. Davis, A. Unterbeck and P. P. Tamburini, *Biochemistry*, 1991, **30**, 10467.
27 K. D. Berndt, P. Güntert, L. P. M. Orbons and K. Wütrich, *J. Mol. Biol.*, 1992, **227**, 757.
28 R. Turner, I. E. Liener and R. E. Lovrien, *Biochemistry*, 1975, **14**, 275.
29 Y. Tsunogae, I. Tanaka, T. Yamane, J. I. Kikkawa, T. Ashida, C. Ishikawa, K. Watanabe, S. Nakamura and K. Takahashi, *J. Biochem. (Tokyo)*, 1986, **100**, 1637.
30 C. W. Chi, F. L. Tan, H. M. Chu, X. Y. Zhang, L. X. Wang, Y. W. Qian, M. L. Wu, G. D. Lin and R. G. Zhang, in *Protease Inhibitors*, eds. A. Takada, M. M. Samama and D. Collen, Elsevier, Amsterdam, 1990, p. 219.
31 M. H. Werner and D. E. Wemmer, *Biochemistry*, 1991, **30**, 3356.
32 M. H. Werner and D. E. Wemmer, *Biochemistry*, 1992, **31**, 999.
33 M. H. Werner and D. E. Wemmer, *J. Mol. Biol.*, 1992, **225**, 873.
34 P. C. Billings and J. M. Habres, *Proc. Natl. Acad. Sci. USA*, 1992, **89**, 3120.
35 N. Nishino, H. Aoyagi, T. Kato and N. Izumiya, *Experientia*, 1975, **31**, 410.
36 S. Terada, K. Sato, T. Kato and N. Izumiya, *Int. J. Pept. Protein Res.*, 1980, **15**, 441.
37 N. Nishino, H. Aoyagi, T. Kato and N. Izumiya, *J. Biochem. (Tokyo)*, 1977, **82**, 901.
38 I. Schechter and A. Berger, *Biochem. Biophys. Res. Commun.*, 1967, **27**, 157.
39 D. Kowalski, T. R. Leary, R. E. McKee, R. W. Sealock, D. Wang and M. Jr. Laskowski, in *Proteinase Inhibitors. Proc. 2nd Int. Res. Conf.*, eds. H. Fritz, H. Tschesche, L. J. Greene and E. Truschett, Springer-Verlag, Berlin, 1974, p. 311.
40 S. Odani and T. Ono, *J. Biochem. (Tokyo)*, 1980, **88**, 1555.
41 T. Kurokawa, S. Hara, H. Takahara, K. Sugawara and T. Ikenaka, *J. Biochem. (Tokyo)*, 1987, **101**, 1361.
42 K. Rolka, G. Kupryszewski, U. Ragnarsson, J. Otlewski, T. Wilusz and A. Polanowski, *Biol. Chem. Hoppe-Seyler*, 1989, **370**, 499.
43 D. I. Maeder, M. Sunde and D. Botes, *Int. J. Peptide Protein Res.*, 1992, **40**, 97.
44 N. Nishino and N. Izumiya, *Biochim. Biophys. Acta*, 1982, **708**, 233.
45 S. Ando, A. Yasutake, M. Waki, N. Nishino, T. Kato and N. Izumiya, *Biochim. Biophys. Acta*, 1987, **916**, 527.
46 V. Pavone, personal communication.
47 A. Dryland and R. C. Sheppard, *J. Chem. Soc., Perkin Trans. 1*, 1986, 125.
48 R. Knorr, A. Trzeciak, A. Bannwarth and D. Gillesen, *Tetrahedron Lett.*, 1989, **30**, 1927.
49 J. P. Tam, C. R. Wu, W. Liu and J. W. Zhang, *J. Am. Chem. Soc.*, 1991, **113**, 6657.
50 W. L. Anderson and C. B. Wetlaufer, *Anal. Biochem.*, 1975, **67**, 493.
51 Worthington Enzymes, Biochemical Products Division, Worthington Diagnostic System, Inc. Freehold, NJ 07728, USA, 1982.
52 U. Piantini, O. W. Sorensen and R. R. Ernst, *J. Am. Chem. Soc.*, 1982, **104**, 6800.
53 A. Bax and D. G. Davis, *J. Magn. Reson.*, 1985, **65**, 355.
54 D. Neuhaus and M. Williamson, in *The Nuclear Overhauser Effect*, VCH, New York, 1989.
55 A. A. Bothner-By, R. L. Stephens, J. Lee, C. D. Warren and R. Jeanloz, *J. Am. Chem. Soc.*, 1984, **106**, 811.
56 C. Griesinger and R. R. Ernst, *J. Magn. Reson.*, 1987, **75**, 261.
57 S. Lifson, A. T. Hagler and P. Dauber, *J. Am. Chem. Soc.*, 1979, **101**, 5111.
58 A. T. Hagler, P. Dauber and S. Lifson, *J. Am. Chem. Soc.*, 1979, **101**, 5131.
59 A. T. Hagler, S. Lifson and P. Dauber, *J. Am. Chem. Soc.*, 1979, **101**, 5122.
60 L. Verlet, *Phys. Rev.*, 1967, **159**, 98.
61 G. Corongiu, M. Aida, M. F. Pas and E. Clementi, in *MOTECC-91: Modern Techniques in Computational Chemistry*, ed. E. Clementi ESCOM, 1991, ch. 21, p. 847.
62 B. R. Brooks, R. F. Bruccoleri, B. D. Olafson, D. J. States, S. Swaminathan and M. Karplus, *J. Comput. Chem.*, 1983, **4**, 187.
63 M. Saviano, M. Aida and G. Corongiu, *Biopolymers*, 1992, **31**, 1017.
64 T. F. Havel and K. Wüthrich, *Bull. Math. Biol.*, 1984, **45**, 665.
65 InsightII User Guide, version 2.1.0 (1992) San Diego: Biosym Technologies.
66 C. L. III Brooks, B. Montgomery Pettitt and M. Karplus, *J. Chem. Phys.*, 1985, **83**, 5897.
67 C. L. III Brooks, in *Proteins: a Theoretical Perspective of Dynamics, Structure and Thermodynamics*, eds. I. Prigogine and S. A. Rice, Wiley, New York, 1988.
68 K. Wütrich, in *NMR of Proteins and Nucleic acids*, Wiley, New York, 1986.
69 O. Jardetzky and G. C. K. Roberts, in *NMR in Molecular Biology*, Academic, New York, 1981.
70 F. C. Bernstein, T. F. Koetzle, G. J. B. Williams, E. F. Meyer, Jr., M. D. Brice, J. R. Rodgers, O. Kennard, T. Shimanouchi and M. Tasumi, *J. Mol. Biol.*, 1977, **112**, 535.
71 E. E. Abola, F. C. Bernstein, S. H. Bryant, T. F. Koetzle and J. Weng, *Protein Data Bank*, in *Crystallographic Databases-Information Content*, Software Systems, Scientist Applications, eds. F. H. Allen, G. Bergerhoff and R. Sievens, Data Commission of the International Union of Crystallography, Bonn, Cambridge, Chester, 1987, p. 107.

Paper 3/06783A
Received 12*th November* 1993
Accepted 4*th January* 1994